Proceedings of the 1998 IEEE
International Conference on Robotics & Automation
Leuven, Belgium • May 1998

Stabilization of the Acrobot via Iterative State Steering*

Alessandro De Luca Giuseppe Oriolo

Dipartimento di Informatica e Sistemistica
Università degli Studi di Roma "La Sapienza"
Via Eudossiana 18, 00184 Roma, Italy
{deluca,oriolo}@labrob.ing.uniroma1.it

Abstract

We present a new approach for the control of the Acrobot, an interesting example of underactuated mechanical system. In particular, our objective is to transfer the system state from the downward equilibrium to the inverted equilibrium position. The proposed method prescribes the execution of three phases. In the first two phases, the robot is preliminarily swung up using an open-loop input and then driven by a suitable feedback to the inverted equilibrium manifold. In the last phase, the Acrobot is steered along this manifold to the inverted equilibrium position, under the action of a robust feedback controller based on the iterative state steering technique. Simulation results are given to show the performance of the method.

1 Introduction

Underactuated robotic systems (i.e., with less controls than generalized coordinates) have recently received increasing attention. The design of mechanisms that can perform complex tasks with less actuators and/or sensors allows to reduce cost, weight and failure rate. On the other hand, innovative approaches are required in order to synthesize effective control strategies.

Examples of underactuated mechanical systems are overhead cranes [1], manipulators with flexible elements [2] and robots with passive joints under gravity, such as the Acrobot [3] and the brachiation robot [4]. The corresponding system equations are highly nonlinear and display a drift term accounting for gravitational or elastic forces. As a consequence, all the above systems are smoothly stabilizable.

Some underactuated mechanisms, however, are not smoothly stabilizable—similarly to the case of kinematic nonholonomic systems. This happens whenever the drift term tends to zero with the generalized velocities. Examples are robots with passive joints in zero gravity [5–7] as well as redundant manipulators driven only through end-effector generalized forces [8].

In principle, systems of the first class can be expected to be easier to control than those of the second. Still, it should be emphasized that a gravitational or elastic drift drastically reduces the region of the state space where the system can be kept in equilibrium. As a consequence, the design of global stabilizers for underactuated systems of the first class becomes a challenging task, often solved by switching between various control phases. A representative instance is the problem of driving the Acrobot from the downward equilibrium to the inverted equilibrium position, which has been addressed by several authors, e.g., see [3, 9–11].

In this paper, we outline a new method for achieving stabilization of the Acrobot in the large. Our control algorithm prescribes the execution of three phases. In the first phase, a swing-up motion is performed in order to achieve a suitable configuration for the second phase, which brings the robot to the inverted equilibrium manifold. Finally, in the third phase, the Acrobot is driven to the inverted equilibrium position by a robust feedback controller designed with the *iterative state steering* (ISS) approach [12]. Such approach has already proved to be successful in the case of nonsmoothly stabilizable underactuated robots [7].

The paper is organized as follows. In the next section, we recall the dynamic equations of the Acrobot and perform some preliminary analysis and manipulation on the model. In Sect. 3, the proposed control method is introduced. Each phase is described in detail and illustrated by simulation. A short discussion on future work is given in the concluding section.

*Work supported by MURST under 40% and 60% funds.

0-7803-4300-x-5/98 $10.00 © 1998 IEEE

2 Model of the Acrobot

The Acrobot is a two-link planar robot moving in the vertical plane, equipped with two revolute joints and a single actuator at the elbow joint (see Fig. 1). For each link, we shall denote by l_i its length, by l_{ci} the distance between its center of mass and the i-th joint axis, by m_i its mass and by J_i its moment of inertia ($i = 1, 2$). The torque at the second joint (the only available input) is indicated by τ.

The equations of motion for this system are

$$b_{11}(q)\ddot{q}_1 + b_{12}(q)\ddot{q}_2 + h_1(q,\dot{q}) + g_1(q) = 0 \quad (1)$$
$$b_{12}(q)\ddot{q}_1 + b_{22}(q)\ddot{q}_2 + h_2(q,\dot{q}) + g_2(q) = \tau, \quad (2)$$

where the elements b_{ij} of the inertia matrix, the velocity terms h_i and the gravitational terms g_i are respectively expressed as

$$\begin{aligned} b_{11}(q) &= a_1 + 2a_2\cos q_2 \\ b_{12}(q) &= a_3 + a_2\cos q_2 \\ b_{22}(q) &= a_3 \\ h_1(q,\dot{q}) &= -a_2 \sin q_2\,(\dot{q}_2^2 - 2\dot{q}_1\dot{q}_2) \\ h_2(q,\dot{q}) &= a_2 \sin q_2\,\dot{q}_1^2 \\ g_1(q) &= a_4\cos q_1 + a_5\cos(q_1+q_2) \\ g_2(q) &= a_5\cos(q_1+q_2), \end{aligned}$$

with

$$\begin{aligned} a_1 &= m_1 l_{c1}^2 + m_2(l_1^2 + l_{c2}^2) + J_1 + J_2 \\ a_2 &= m_2 l_1 l_{c2} \\ a_3 &= m_2 l_{c2}^2 + J_2 \\ a_4 &= g(m_1 l_{c1} + m_2 l_1) \\ a_5 &= g m_2 l_{c2}. \end{aligned}$$

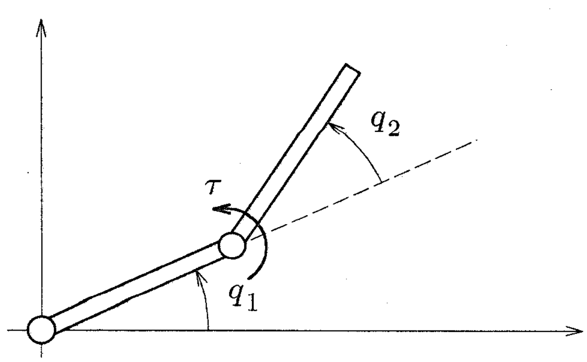

Figure 1: The Acrobot: a planar robot in the vertical plane with a single actuator at the elbow joint

2.1 Equilibrium manifold

Beyond the unforced equilibria $x_l = (-\pi/2, 0, 0, 0)$ (*lower* equilibrium) and $x_u = (\pi/2, 0, 0, 0)$ (*upper* or *inverted* equilibrium), the Acrobot has a manifold of forced equilibrium points. In particular, the robot is at rest whenever $\dot{q}_1$, $\dot{q}_2$ and $g_1(q)$ are zero and the joint torque τ is such to equalize g_2 in eq. (2). The equation of the equilibrium manifold, which will be denoted by Ψ, can thus be written as

$$\psi(q) = a_4\cos q_1 + a_5\cos(q_1+q_2) = 0, \quad (3)$$

while the torque needed to keep the system in equilibrium is

$$\tau_{\text{eq}} = g_2(q) = a_5\cos(q_1+q_2). \quad (4)$$

It can be easily proven that the equilibrium manifold is not connected. In fact, physical intuition immediately suggests that Ψ splits into a *lower* submanifold Ψ_l and an *upper* or *inverted* submanifold Ψ_u, which do not intersect. The two are characterized by negative and positive values of q_1, respectively. In particular, the lower equilibrium belongs to Ψ_l, while the inverted equilibrium belongs to Ψ_u. The latter fact will be exploited to achieve our control objective.

2.2 Partial feedback linearization

When addressing the control problem for underactuated mechanical systems, it is often convenient to perform a partial feedback linearization [7, 8, 9] of the dynamic model. To this end, define the state vector $x = (q_1, q_2, \dot{q}_1, \dot{q}_2)$, and choose the second joint torque as

$$\tau = \tilde{b}_{22}(q)u + \tilde{h}_2(q,\dot{q}) + \tilde{g}_2(q), \quad (5)$$

where u is an auxiliary input and

$$\begin{aligned} \tilde{b}_{22} &= b_{22} - b_{12}^2/b_{11} \\ \tilde{h}_2 &= h_2 - b_{12}h_1/b_{11} \\ \tilde{g}_2 &= g_2 - b_{12}g_1/b_{11}. \end{aligned}$$

Using eqs. (1–2), it is easy to verify that the state-space model takes the form

$$\dot{x}_1 = x_3 \quad (6)$$
$$\dot{x}_2 = x_4 \quad (7)$$
$$\dot{x}_3 = \tilde{f}_{x3}(x) + \tilde{g}_{x3}(x)u \quad (8)$$
$$\dot{x}_4 = u. \quad (9)$$

with the appropriate expressions for $\tilde{f}_{x3}$ and $\tilde{g}_{x3}$.

With the above technique, it is straightforward to design u so as to obtain a desired evolution for q_2. Setting $u = 0$ in eq. (5) automatically yields the equilibrium joint torque (4), for $\dot{q} = 0$ and on the manifold (3).

3 The propósed control strategy

Our objective is to drive the Acrobot from the lower equilibrium position x_l to the inverted equilibrium position x_u. The proposed control strategy prescribes the execution of three phases:

1. swing-up motion;
2. stabilization to Ψ_u;
3. iterative steering to x_u.

Roughly speaking, in the first phase the second link undergoes a periodic motion aimed at bringing the first link in a generic upward position. When this has been achieved, a stabilizing control takes over, whose objective is to lead the robot to the inverted equilibrium manifold Ψ_u. Finally, the ISS technique is applied in the third phase to drive the Acrobot along Ψ_u to the inverted equilibrium x_u. In the following, each phase is discussed in detail and illustrated by simulation.

3.1 Swing-up motion

Spong and co-authors have proposed various methods for performing the swing-up phase [9, 11]. All these rely on a partial feedback linearization of the model (like the one used in Sect. 2.2) and exploit the instability of the resulting zero dynamics. Particular care is given to the case in which q_2 is constrained to lie in an interval $[q_2^{\min}, q_2^{\max}]$ due to joint limits.

In our case, a simpler swing-up strategy was sufficient, because we assume that no limit exists for the rotation of the second link. Moreover, while in [9, 11] the objective of the swing-up phase is to bring the Acrobot inside the (small) basin of attraction of an LQR controller—designed so as to provide balancing around the inverted equilibrium position—we only require the first link to point upwards at the end of this phase. Hence, the state space region in which the control can be switched to the second phase is quite large.

We choose input u in eqs. (6–9) as

$$u(t) = \bar{u}\cos\omega t, \qquad \bar{u}, \omega \in I\!R. \tag{10}$$

In view of (7) and (9), the evolution of q_2 is a cosine wave itself, while $q_1(t)$ is obtained by forward integration of (6) and (8). Given the dynamic parameters of the Acrobot, it is easy to choose the constants $\bar{u}$ and ω so as to swing q_1 in the first or fourth quadrant. Note that the expressions of $\tilde{f}_{x3}$, $\tilde{g}_{x3}$ in (8) are not needed to compute τ. Only $\tilde{b}_{22}$, $\tilde{h}_2$ and $\tilde{g}_2$ must be available to implement the input (10) via (5).

The condition for switching to the second phase is

$$q_1(t_{\rm I}) \in (0, \pi) \quad (\bmod 2\pi),$$

where $t_{\rm I}$ denotes the corresponding switching instant. However, it is desirable that joint velocities are not too large at $t = t_{\rm I}$, for this would result in a longer duration and worse behavior of the second phase (see Sect. 3.2). More sophisticated, provably convergent swing-up strategies can be designed following [9].

3.1.1 Simulation

In simulation, we have used the following parameters: $l_1 = l_2 = 1$ m, $l_{c1} = l_{c2} = 0.5$ m, $m_1 = m_2 = 1$ kg, $J_1 = 0.2, J_2 = 1$ kg·m^2. During the swing-up phase, torque τ is given by (5) and (10), where $\bar{u} = 6$ and $\omega = 1$ rad/sec. Results are shown in Figs. 2–3. Note that the second joint undergoes almost two complete rotations, while the first joint angle becomes positive after approximately 2.3 seconds. However, the swing-up phase is terminated at $t_{\rm I} = 3$ s, because an additional low velocity requirement was included in the switching condition.

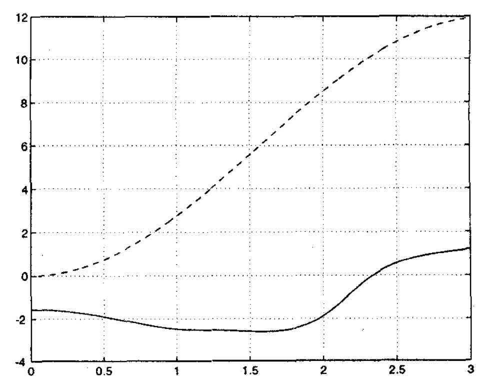

Figure 2: Position of the first (solid) and second (dashed) joint during the first phase (rad)

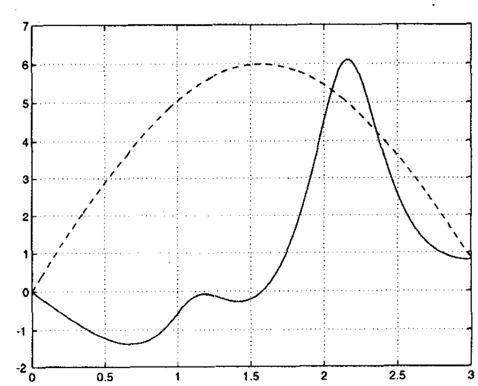

Figure 3: Velocity of the first (solid) and second (dashed) joint during the first phase (rad/sec)

3.2 Stabilization to Ψ_u

In the second phase, the Acrobot must be driven to the inverted equilibrium manifold Ψ_u. To compute a suitable controller, it is convenient to perform the following change of coordinates

$$z = \begin{pmatrix} z_1 \\ z_2 \\ z_3 \\ z_4 \end{pmatrix} = \begin{pmatrix} \psi(q) \\ q_2 \\ \dot{\psi}(q, \dot{q}) \\ \dot{q}_2 \end{pmatrix}.$$

We obtain

$$\begin{aligned} \dot{z}_1 &= z_3 \\ \dot{z}_2 &= z_4 \\ \dot{z}_3 &= f_{z3}(z) + g_{z3}(z)\tau \\ \dot{z}_4 &= f_{z4}(z) + g_{z4}(z)\tau, \end{aligned}$$

where the expressions of f_{z3}, g_{z3}, f_{z4} and g_{z4} can be computed from eqs. (1–2) and from the expression (3) of $\psi(q)$. Setting

$$\tau = -\frac{f_{z3}(z)}{g_{z3}(z)} + \frac{v}{g_{z3}(z)}, \tag{11}$$

with v an auxiliary input, the transformed dynamics is partially linearized as

$$\begin{aligned} \dot{z}_1 &= z_3 \\ \dot{z}_2 &= z_4 \\ \dot{z}_3 &= v \\ \dot{z}_4 &= \tilde{f}_{z4}(z) + \tilde{g}_{z4}(z)v, \end{aligned}$$

with the appropriate expressions for $\tilde{f}_{z4}$ and $\tilde{g}_{z4}$. Therefore, by setting in eq. (11)

$$v = -k_p z_1 - k_d z_3 = -k_p \psi - k_d \dot{\psi}, \tag{12}$$

with $k_p, k_d > 0$, $\psi(t)$ will converge to zero exponentially. Hence, the Acrobot will complete the approach phase to the equilibrium manifold Ψ quite fast.

Some remarks are in order at this point.

- Like in the first phase, it is sufficient to compute f_{z3} and g_{z3}—whose expressions are not given here for lack of space—in order to implement the proposed controller (12) through eq. (11).
- As the first link points upwards at the end of the swing-up, it can be proven that the Acrobot will be driven to the inverted equilibrium manifold Ψ_u (and not to the lower equilibrium manifold Ψ_l).
- While the convergence of z_1, z_3 to zero is guaranteed, it would be necessary to analyze the stability of the residual zero dynamics, i.e., the evolution of z_2, z_4. At the present stage of our investigation, this issue has not been addressed, because q_2 is allowed to rotate freely. However, such a study—which can be performed along the lines of [9]—is mandatory before experimental validation of the proposed approach is attempted. In principle, convergence to the inverted equilibrium manifold with internal stability can be achieved following the *nonlinear regulation* method [13].

In the implementation, the second phase is terminated at the time instant $t_{\rm II}$ in which the norm of $(\psi, \dot{\psi})$ falls below a given threshold. At this point, the iterative steering phase is started.

3.2.1 Simulation

The second phase has been simulated from time instant $t_{\rm I}$ and robot state $x(t_{\rm I})$ achieved at the end of the swing up. The second joint torque τ is computed by eq. (11), with v as in (12) and $k_p = k_d = 4$.

Joint positions and velocities are respectively given in Figs. 4 and 5, while Fig. 6 shows the evolution of the norm of $(\psi, \dot{\psi})$ during the approach to the inverted equilibrium manifold. The termination condition was met at $t_{\rm II} = 6.25$ s.

Note that, although $\dot{\psi}$ is virtually zero at $t_{\rm II}$, there are still residual velocities at the joints. This is not surprising, for nonzero velocities tangent to manifold Ψ_u (i.e., satisfying $\dot{\psi}(q, \dot{q}) = 0$) are allowed.

3.3 Iterative steering to x_u

To design a controller that drives the Acrobot to x_u along the inverted equilibrium manifold Ψ_u, we adopt the *iterative state steering* (ISS) approach [12], which represents a fairly general framework for the robust stabilization of controllable nonlinear systems.

In general, given a desired equilibrium x_d for the system, the basic tool for applying this technique is a contractive command $u = u(x, x_0, x_d, t_s, t)$, i.e., a control that can steer the system in a finite time t_s from an arbitrary initial state x_0 to a final state $x(t_s)$ which is closer to x_d. The iterative application of such law (obtained by resetting every t_s seconds the initial state to the current state) yields a time-varying feedback control that makes x_d exponentially stable, provided that the closed-loop dynamics within each iteration is Lipschitz with respect to x and that the (typically, open-loop) control u is continuous with respect to the initial state x_0.

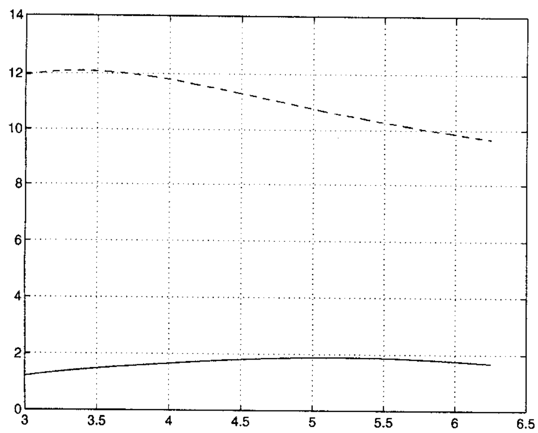

Figure 4: Position of the first (solid) and second (dashed) joint during the second phase (rad)

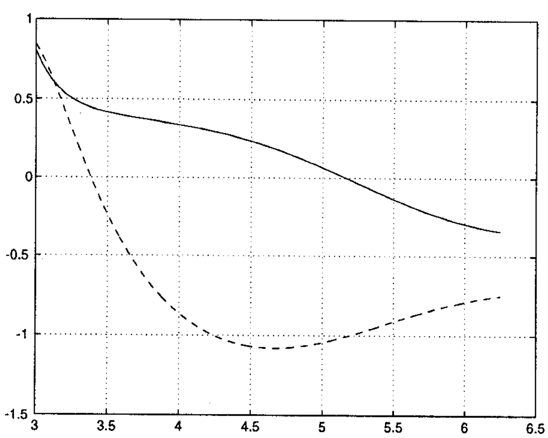

Figure 5: Velocity of the first (solid) and second (dashed) joint during the second phase (rad/sec)

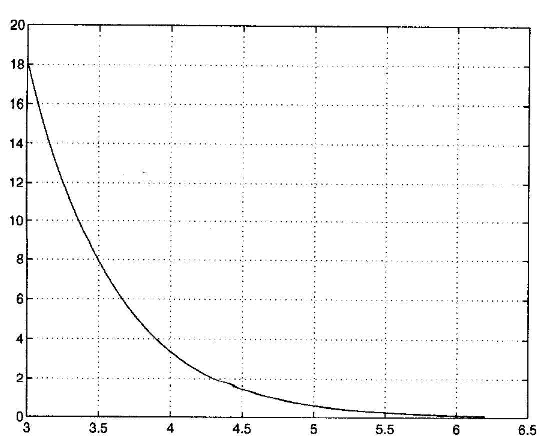

Figure 6: Norm of $(\psi, \dot{\psi})$ during the second phase

One remarkable feature of the above approach is that the obtained controller is inherently robust. In fact, it can be shown that small non-persistent perturbations of the model are rejected, while ultimately bounded errors arise in the presence of persistent perturbations. We have already applied this method successfully to nonholonomic mobile robots [12] and underactuated manipulators in zero gravity [7].

In the present case, the ISS paradigm suggests the following algorithm for stabilizing the Acrobot to x_u. The algorithm is started from time instant $t_{\rm II}$ and robot state $x(t_{\rm II})$ at which the second phase is terminated.

Step 0 Set $t^0_{\rm III} = t_{\rm II}$, $t^1_{\rm III} = t_{\rm II} + t_s$, $x_0 = x(t_{\rm II})$ and $k = 1$.

Step 1 Select a point x_k on the equilibrium manifold Ψ_u. Point x_k should be closer to x_u than x_{k-1}, but sufficiently close to x_{k-1} itself.

Step 2 Derive the approximate linearization of system (6–9) at the equilibrium point x_k.

Step 3 Compute a control $u = u(x, x_{k-1}, x_k, t_s, t)$ that steers the state of the linearized system from x_{k-1} to x_k in $[t^{k-1}_{\rm III}, t^k_{\rm III}]$. Once this control is applied to the original system (6–9), its final state will be in general $\tilde{x}_k \neq x_k$.

Step 4 Set $t^k_{\rm III} = t^{k-1}_{\rm III} + t_s$, $x_k = \tilde{x}_k$, $k = k + 1$ and go to Step 1.

Below, we detail steps 1–3 of the algorithm.

Step 1

Given x_{k-1}, choose the second component of x_k as

$$q_{k,2} = q_{k-1,2} + \sigma(q_{d,2} - q_{k-1,2}), \qquad \sigma \in (0,1), \quad (13)$$

where $q_{d,2} = 0 \pmod{2\pi}$. To guarantee that x_k belongs to Ψ_u, its first component is computed from eq. (3) as

$$q_{k,1} = \arctan\left(\frac{a_4 + a_5 \cos q_{k,2}}{a_5 \sin q_{k,2}}\right), \qquad (14)$$

and we let

$$\dot{q}_{k,1} = \dot{q}_{k,2} = 0. \qquad (15)$$

It is easy to verify that, with the above choice, x_k is closer (in norm) to x_u than x_{k-1}. The requirement that x_k is sufficiently close to x_{k-1} can be met by taking σ small enough. ◇

Step 2

Letting $\xi_k = x - x_k$, the approximate linearization of system (6–9) at the equilibrium point $x_k \in \Psi_u$ is obtained as

$$\dot{\xi}_k = A_k \xi_k + B_k u, \tag{16}$$

where

$$A_k = \begin{pmatrix} 0 & 0 & 1 & 0 \\ 0 & 0 & 0 & 1 \\ A_{k,31} & A_{k,32} & 0 & 0 \\ 0 & 0 & 0 & 0 \end{pmatrix} \quad B_k = \begin{pmatrix} 0 \\ 0 \\ B_{k,3} \\ 1 \end{pmatrix},$$

being

$$\begin{aligned} A_{k,31} &= \frac{a_4 \sin q_{k,1} + a_5 \sin(q_{k,1} + q_{k,2})}{a_1 + 2a_2 \cos q_{k,2}} \\ A_{k,32} &= \frac{a_5 \sin(q_{k,1} + q_{k,2})}{a_1 + 2a_2 \cos q_{k,2}} \\ B_{k,3} &= -\frac{a_3 + a_2 \cos q_{k,2}}{a_1 + 2a_2 \cos q_{k,2}}. \end{aligned}$$

A straightforward calculation shows that the above linear system is always controllable on Ψ_u. ◇

Step 3

In order to steer the linearized system (16) from $\xi_k(t_{\rm III}^{k-1}) = x_{k-1} - x_k$ to the origin in $t_s = t_{\rm III}^{k} - t_{\rm III}^{k-1}$, a *terminal* controller can be used [14, Sect. 9.2.1]

$$u(t) = B_k F_k (x - x_k) + B_k^{\rm T} e^{-\tilde{A}_k^{\rm T}(t - t_{\rm III}^{k-1})} G_k^{-1} (x_k - x_{k-1}), \tag{17}$$

where F_k makes $\tilde{A}_k = A_k + B_k F_k$ asymptotically stable and G_k^{-1} is the inverse of the *controllability Gramian*

$$G_k(\tilde{A}_k, B_k, t_s) = \int_0^{t_s} e^{-\tilde{A}_k \tau} B_k B_k^{\rm T} e^{-\tilde{A}_k^{\rm T} \tau} d\tau.$$

It is immediate to show that, with the control law (17), the closed-loop dynamics within each iteration is Lipschitz with respect to x and continuous at zero with respect to x_k, thereby guaranteeing the applicability of the iterative steering paradigm.

The rationale for the presence of the first term—a simple linear stabilizing feedback—in the control input (17) is twofold. First, this gives a better conditioning of the controllability Gramian G; second, we would like the state of system (6–9) during the steering interval $[t_{\rm III}^{k-1}, t_{\rm III}^{k}]$ to remain close to x_k—and hence, in the region of validity for the linearization (16). ◇

With the above algorithm, exponential stability of x_u is guaranteed. This property is global: the Acrobot will be driven to the inverted equilibrium position for any initial state on manifold Ψ_u (in practice, any state sufficiently close to Ψ_u will be acceptable). Also, the obtained convergence is quite robust: non-persistent perturbations are rejected, whereas ultimately bounded errors arise under persistent disturbances.

3.3.1 Simulation

The third phase has been simulated from time instant $t_{\rm II}$ and robot state $x(t_{\rm II})$ achieved at the end of the second phase. We have chosen $t_s = 2$, and selected the desired state x_k at the end of each iteration according to eqs. (13–15), with $\sigma = 0.3$. Within each iteration, control u is computed by eq. (17) (with the poles of $\tilde{A}_k$ constantly placed at $(-2, -3, -4, -5)$) and joint torque τ is obtained by plugging u in eq. (5).

The joint evolution is given in Figs. 7–8. Note that the second joint converges to the equilibrium angle $q_{d,2} = 4\pi = 0 \pmod{2\pi}$, conveniently 'wrapped' in order to take into account the value of q_2 at the end of the second phase. A logarithmic plot of the joint error norm, shown in Fig. 9, confirms the exponential convergence to the desired equilibrium.

The pronounced oscillations exhibited during the first two iterations are due to the fact that the contraction phase is started with nonzero joint velocities (see Fig. 5). This affects the performance of the terminal controller (17), which is computed on the basis of the approximate linearization (16), where $\dot{q}_1$ and $\dot{q}_2$ are assumed to be zero (an improvement would be to linearize the system around states on Ψ_u with nonzero velocity). Nevertheless, the ISS technique was able to drive the Acrobot to the inverted equilibrium position.

4 Conclusions

An innovative approach was presented for stabilizing the Acrobot, an interesting example of underactuated mechanical system. The control algorithm prescribes the execution of three phases. In the first two phases, the Acrobot is preliminarily swung up by a periodic input and then driven to the inverted equilibrium manifold Ψ_u via a suitable feedback. In the third phase, the robot is steered to the inverted equilibrium position x_u traveling along Ψ_u. The time-varying feedback used in this phase was designed following the iterative state steering approach, which we already applied successfully to other underactuated systems [7, 12].

The present work is to be regarded as a preliminary report of our investigation. Issues that deserve further study are the stability of the zero dynamics in the first two phases as well as a complete assessment of the robustness properties of the third phase under realistic perturbations. In the same spirit, it would be interesting to attempt the design of less model-based control laws for executing the first and the second phase.

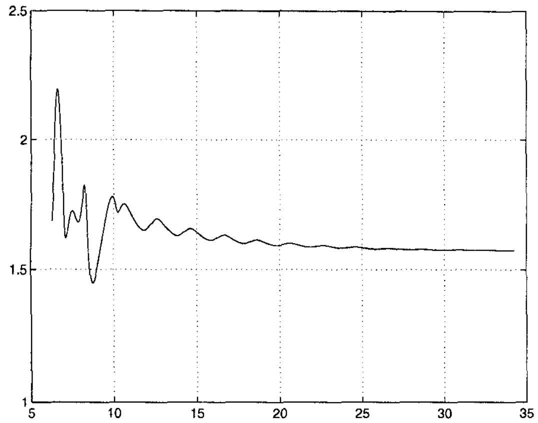

Figure 7: Position of the first joint during the third phase (rad)

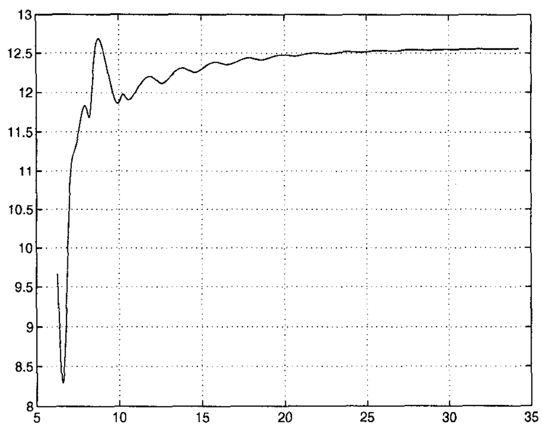

Figure 8: Position of the second joint during the third phase (rad)

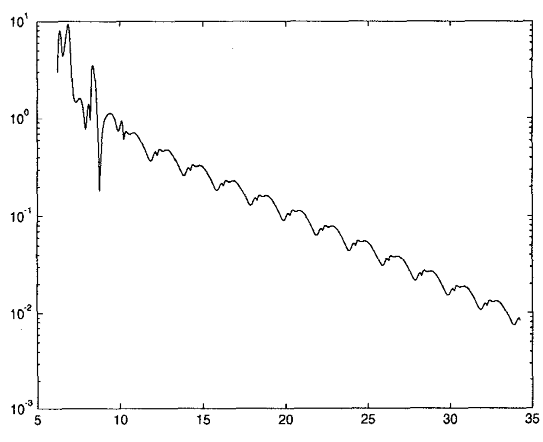

Figure 9: Logarithmic plot of the joint error norm during the third phase

References

[1] B. d'Andréa-Novel, F. Boustany, F. Conrad, and B. P. Rao, "Feedback stabilization of a hybrid PDE-ODE system: Application to an overhead crane," *Mathematics of Control, Signals, and Systems*, vol. 7, pp. 1–22, 1994.

[2] D. Seto and J. Baillieul, "Control problems in super-articulated mechanical systems," *IEEE Trans. on Automatic Control*, vol. 39, no. 12, pp. 2442–2453, 1994.

[3] R. M. Murray and J. Hauser, "A case study in approximate linearization: The Acrobot example" Memo. No. UCB/ERL M91/46, University of California at Berkeley, 1991.

[4] F. Saito, T. Fukuda, and F. Arai, "Swing and locomotion control for two-link brachiation robot," *1993 IEEE Int. Conf. on Robotics and Automation*, pp. 719–724, 1993.

[5] G. Oriolo and Y. Nakamura, "Control of mechanical systems with second-order nonholonomic constraints: Underactuated manipulators," *30th IEEE Conf. on Decision and Control*, pp. 2398–2403, 1991.

[6] T. Suzuki, M. Koinuma, and Y. Nakamura, "Chaos and nonlinear control of a nonholonomic free-joint manipulator," *1996 IEEE Int. Conf. on Robotics and Automation*, pp. 2668–2675, 1996.

[7] A. De Luca, R. Mattone, and G. Oriolo, "Stabilization of underactuated robots: Theory and experiments for a planar 2R manipulator," *1997 IEEE Int. Conf. on Robotics and Automation*, pp. 3274–3280, 1997.

[8] A. De Luca, R. Mattone, and G. Oriolo, "Dynamic mobility of redundant robots using end-effector commands," *1996 IEEE Int. Conf. on Robotics and Automation*, pp. 1760–1767, 1996.

[9] M. W. Spong, "The swing up control problem for the Acrobot," *IEEE Control Systems*, vol. 15, no. 1, pp. 49–55, 1995.

[10] D. E. Davison and S. A. Bortoff, "Regulation of the Acrobot," *1995 IFAC Symp. on Nonlinear Control Systems Design*, pp. 390–395, 1995.

[11] M. W. Spong and L. Praly, "Control of underactuated mechanical systems using switching and saturation," *Proc. of the Block Island Work. on Control using Logic Based Switching*, Springer-Verlag, 1996.

[12] P. Lucibello and G. Oriolo, "Stabilization via iterative state steering with application to chained-form systems," *35th IEEE Conf. on Decision and Control*, pp. 2614–2619, 1996.

[13] A. Isidori, *Nonlinear Control Systems*, 3rd Edition, Springer-Verlag, 1995.

[14] T. Kailath, *Linear Systems*. Prentice-Hall, Englewood Cliffs, NJ, 1980.